

Magnesium ion conducting polyvinyl alcohol–polyvinyl pyrrolidone-based blend polymer electrolyte

Mangalam Ramaswamy¹ · Thamilselvan Malayandi² ·
Selvasekarapandian Subramanian³ · Jayakumar Srinivasalu¹ ·
Manjuladevi Rangaswamy⁴

Received: 14 August 2016 / Revised: 9 January 2017 / Accepted: 10 February 2017 / Published online: 22 February 2017
© Springer-Verlag Berlin Heidelberg 2017

Abstract Structural, thermal, electrical and electrochemical behaviour of polymer blend electrolytes comprising polyvinyl alcohol (PVA) and polyvinyl pyrrolidone (PVP) as host polymers and $\text{Mg}(\text{ClO}_4)_2$ as dopant salt have been investigated. The changes in the structural properties on the incorporation of dopant in the blends were investigated by XRD and FTIR analyses. Thermal properties of pure PVA–PVP blend and their complexes were examined by DSC to measure how the thermal transitions of the prepared films were affected by different concentration of $\text{Mg}(\text{ClO}_4)_2$. The ionic conductivity and dielectric behaviour were explored using A.C. impedance spectroscopy. The trend of ionic conductivity increases almost proportionally to the content of magnesium salt and can be related to an increase of amorphous phase at high level of dopant salt. The electrochemical stability of the optimum conducting blend polymer electrolyte is found to be ~ 3.5 V. The Mg^{2+} transference number for the sample with optimized conductivity was found to be 0.31.

Keywords Blend polymer · Magnesium ion · Ionic conductivity · Transient cross-linking knots · Cyclic voltammetry

✉ Selvasekarapandian Subramanian
sekarapandian@rediffmail.com

¹ Department of Physics, PSG Institute of Technology and Applied Research, Coimbatore, Tamil Nadu 641062, India

² Department of Physics, Thanthai Periyar Government Institute of Technology, Vellore, Tamil Nadu 632002, India

³ Materials Research Center, Coimbatore 641045, India

⁴ Department of Physics, SriGuru Institute of Technology, Coimbatore, Tamil Nadu 641110, India

Introduction

Research on rechargeable magnesium ion battery has spurred intense interest among researchers in industry and academia in the recent past due to the following factors: (i) superior volumetric capacity 3833 mAh cm^{-3} than that for Li metal (2046 mAh cm^{-3}) and (ii) non-dendritic Mg metal anode. Despite its advantages, the development of Mg rechargeable batteries has been limited by several bottlenecks: (i) kinetically torpid Mg^{2+} insertion into ion-transfer hosts due to the strong polarization effect of the small divalent Mg^{2+} and (ii) lack of appropriate non-aqueous media that conduct Mg^{2+} ions [1, 2]. However, passivation-free situation for Mg electrodes exists indeed in Grignard solutions (RMgX in ethers, R = organic alkyl or aryl group and X = halide like Cl^- or Br^-). Yet, the commercialization of those batteries using Grignard reagents was not successful in view of (i) low anodic stability, (ii) too narrow voltage window and (iii) low ionic conductivity. In addition, ionic liquids (ILs) have been investigated for the preparation of electrolytes for magnesium batteries as they possess high ionic conductivity and low vapour pressure and are non-flammable [3, 4]. However, it has been reported that Mg electrodes are generally reactive towards imidazolium-based ILs. Thus, an ideal electrolyte system with sufficiently high ionic conductivity, wider electrochemical stability and non-flammable is highly desirable for ultimate industrialization of Mg secondary batteries [5, 6].

Polymer salt complexes are of scientific interest because they combine ionic conductivity with solid and they are yet flexible, making them a suitable candidate for its possible application in different devices such as energy conversion, electrochromic displays and photo-electrochemical solar cells. A number of methods are available in literature to modify the structure of the polymer electrolytes in order to improve their electrical, electrochemical and mechanical properties. These

approaches include grafting of polymers, cross-linking two polymers, blending of two polymers [7], adding plasticizers to polymer electrolytes [8, 9] and adding inorganic inert filler to make composite polymer electrolytes [10]. Among these approaches, polymer blending is a useful technique for the development of new polymeric materials with extended properties beyond the range that can be obtained from single polymer equivalents.

Literature provides details about blending polyvinyl alcohol (PVA)/polyvinyl pyrrolidone (PVP), PVA/starch and PVA/PAN polymer electrolytes with lithium and ammonium salts [11–15]. Data concerning polymer blend with magnesium salts are scanty [16, 17]. The present scope of the study is to prepare solid blend polymer electrolyte film consisting of PVA, PVP and $\text{Mg}(\text{ClO}_4)_2$ for various concentrations of magnesium salt by keeping PVA/PVP blend ratio as a constant (50 mol%:50 mol%), in order to optimize the dopant concentration which could give the maximum conductivity at room temperature. The polymer–polymer interaction, its miscibility and the hydrogen bonding between the PVA and PVP have been already reported in literature [18–20]. Since both the polymers PVA and PVP are soluble in water and miscible in all proportions, and have polar side groups (hydroxyl and nitrogen groups, respectively), they assist the film formation as a result of the attractive interaction between the polymer chains and cations/anions. PVA is a semi-crystalline polymer with very high dielectric strength ($>1000 \text{ kV mm}^{-1}$), good charge storage capacity, high tensile strength, abrasion resistance and dopant-dependent electrical and optical properties [21]. PVP is a bio-compatible polymer possessing a very high T_g (359 K) due to the presence of the rigid pyrrolidone group.

In the present study, impedance spectroscopy is employed to understand the ion transport behaviour, micro-Brownian motion of the polymer chains, ionic conduction and electrode polarization effects [22–24]. In order to understand the

structural alteration and thermal transition that takes place in the blend polymer electrolyte system, the samples have been subjected to X-ray diffraction (XRD), Fourier transform infrared spectroscopy (FTIR), differential scanning calorimetry (DSC), complex impedance spectroscopy, transport number measurements, linear sweep voltammetry (LSV) and cyclic voltammetry (CV) measurements.

Experimental procedure

PVA (88% hydrolysed) with an average molecular weight (1,25,000, Sd Fine), PVP with an average molecular weight (40,000, Merck) and magnesium perchlorate ($\text{Mg}(\text{ClO}_4)_2$ (Merck) were used as the starting materials. Blend polymer electrolytes (BPE) of different compositions of PVA/PVP/ $\text{Mg}(\text{ClO}_4)_2$ have been prepared by solution casting technique using double-distilled water as the solvent. The composition details are given in Table 1. PVA was initially added to the solvent at 50 °C and stirred continuously until the complete dissolution of the polymer in the solvent. Appropriate quantity of PVP is then added to the solution and stirred continuously to get a clear solution. After the dissolution of the polymer PVP in the solvent, required quantity of $\text{Mg}(\text{ClO}_4)_2$ was added and the resultant solution was stirred continuously until a clear homogeneous solution is obtained. The solution was then poured to polypropylene petri dishes and allowed to dry in air at room temperature for 7 days. Utmost care was taken to remove the residual traces of the water molecules by drying the films in air oven at 80 °C for 72 h and then for 80 °C for 48 h in vacuum oven. This procedure yields mechanically stable, free standing films of thickness between 187 and 190 μm . The obtained films were stored in vacuum desiccators to avoid moisture absorption until further use. Figure 1

Table 1 Sample code, composition, FTIR band assignments, ionic conductivity (σ), activation energy (E_a), total ionic transference number (t_{ion}) and cationic transference number ($t_{\text{Mg}^{2+}}$) for BPEs with different concentrations of $\text{Mg}(\text{ClO}_4)_2$

Sample code	Composition	FTIR band assignments (cm^{-1})					$\sigma \text{ S cm}^{-1}$ (303 K)	E_a	R	t_{ion}	$t_{\text{Mg}^{2+}}$
		OH stretching	CH_2 asymmetric stretching	C=O stretching	C–O stretching	ClO_4^- stretching					
50:50	50 m% PVA-50 m% PVP	3327	2938	1655	1091	–	–	–	–	–	–
50:50:5	50 m% PVA-50 m% PVP: 5 m% $\text{Mg}(\text{ClO}_4)_2$	3325	2922	1655	1099	622	1.9×10^{-8}	0.71	0.95	0.95	0.07
50:50:10	50 m% PVA-50 m% PVP: 10 m% $\text{Mg}(\text{ClO}_4)_2$	3322	2924	1647	1088	622	8.5×10^{-8}	0.68	0.96	0.95	0.14
50:50:15	50 m% PVA-50 m% PVP: 15 m% $\text{Mg}(\text{ClO}_4)_2$	3322	2922	1642	1088	622	2.6×10^{-7}	0.62	0.98	0.96	0.22
50:50:20	50 m% PVA-50 m% PVP: 20 m% $\text{Mg}(\text{ClO}_4)_2$	3319	2922	1642	1086	622	1.7×10^{-5}	0.46	0.99	0.98	0.29
50:50:25	50 m% PVA-50 m% PVP: 25 m% $\text{Mg}(\text{ClO}_4)_2$	3322	2922	1642	1069	622	1.1×10^{-4}	0.34	0.99	0.98	0.31

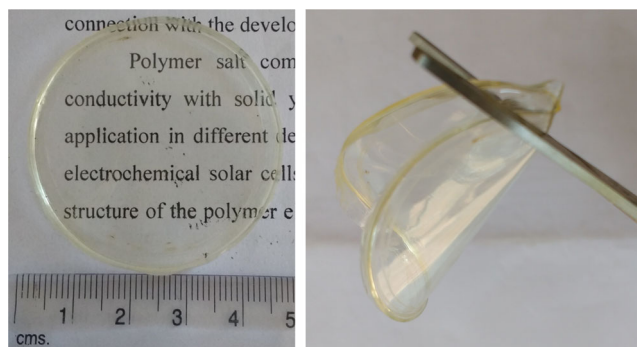


Fig. 1 Image of 50 mol% PVA + 50 mol% PVP + 25 mol% $\text{Mg}(\text{ClO}_4)_2$

shows the photograph of BPE of typical composition 50 mol% PVA + 50 mol% PVP + 25 mol% $\text{Mg}(\text{ClO}_4)_2$.

XRD scans were taken using Philips X'Pert PRO diffractometer at room temperature. The diffraction peaks were recorded at Bragg's angle (2θ) in the range of 10° to 80° . The blend polymer electrolytes were subjected to FTIR study using Shimadzu 8000 spectrophotometer in the wave number ranging 400 – 4000 cm^{-1} . The melting temperature of the solid polymer electrolytes was obtained from DSC measurements using a MAS-5800 model DSC 200 differential scanning calorimeter in N_2 atmosphere with a heating rate of $10\text{ }^\circ\text{C min}^{-1}$. The electrical conductivity of the polymer electrolytes was evaluated using impedance spectroscopy using a HIOKI 3532 LCR impedance analyser interfaced with a computer in the frequency range of 42 Hz – 5 MHz for all the samples in the temperature range 303 to 343 K with stainless steel (SS) as the blocking electrodes. The Mg^{2+} ion transport number of the BPE was evaluated using a combination of A.C. impedance spectroscopy and D.C. polarization technique proposed by Evans et al. Cyclic voltammograms (CV) of the symmetrical cells were recorded using potentiostat/galvanostat (EG&G PARC Model Versastat) at a scan rate of 5 mV s^{-1} . The electrochemical stability of the BPE was evaluated by means of linear sweep voltammetry (LSV) using stainless steel (SS) as the working electrode and magnesium disk as the combined counter and reference electrode.

Results and discussion

XRD analysis

The X-ray diffractograms of pure $\text{Mg}(\text{ClO}_4)_2$ and undoped and doped PVA/PVP blend polymer electrolytes containing different mole ratios of magnesium perchlorate are shown in Fig. 2. A single broad peak observed around $2\theta = 20^\circ$ is attributed to the amorphous nature of the polymer electrolytes. It is observed from the spectra that the intensity of the peak decreases with increasing dopant concentration. Also, the shifting and broadening of this peak with increasing dopant

concentration indicate the interaction of $\text{Mg}^{2+}/\text{ClO}_4^{2-}$ with the polar side groups of the polymers. This interaction will disrupt the long range order of the polymer chains which may be considered as the reason for the increased amorphicity of the BPEs [25]. Further, there were no extra peaks corresponding to $\text{Mg}(\text{ClO}_4)_2$ in the BPEs evidencing the complete dissolution of the salt in the polymer matrix.

FTIR analysis

FTIR spectroscopy is an important tool for the investigation of the information pertaining to ion–polymer interaction. In the present study, FTIR spectroscopy is used to establish interactions between the polymer PVA/PVP and $\text{Mg}(\text{ClO}_4)_2$. When $\text{Mg}(\text{ClO}_4)_2$ is incorporated in the polymer matrix, we expect prominent changes mainly in the regions namely (i) 3300 – 3200 cm^{-1} (O–H stretching vibration mode of PVA), (ii) 1600 – 1650 cm^{-1} (C=O stretching vibration of PVP), (iii) 1100 – 1000 cm^{-1} (C–O stretching of PVA) and (iv) 622 cm^{-1} (ClO_4^- stretching), while the other vibrational bands may not be affected much. FTIR spectra of pure PVA–PVP and PVA/PVP/ $x\text{ Mg}(\text{ClO}_4)_2$ ($x = 5, 10, 15, 20$ and $25\text{ mol}\%$) BPEs are presented in Fig. 3. The vibrational band appearing around 3327 cm^{-1} in the FTIR spectra corresponds to the OH stretching of pure PVA (Fig. 3 (a)). On addition of $\text{Mg}(\text{ClO}_4)_2$ in the polymer matrix, shifting in the wave number had been observed (Fig. 3 (a–f)) which indicates that there is complex formation between the hydroxyl group of PVA and the cations of the dopant [11]. The band appearing around 1655 cm^{-1} in pure PVA–PVP which is assigned to C=O stretching of PVP is

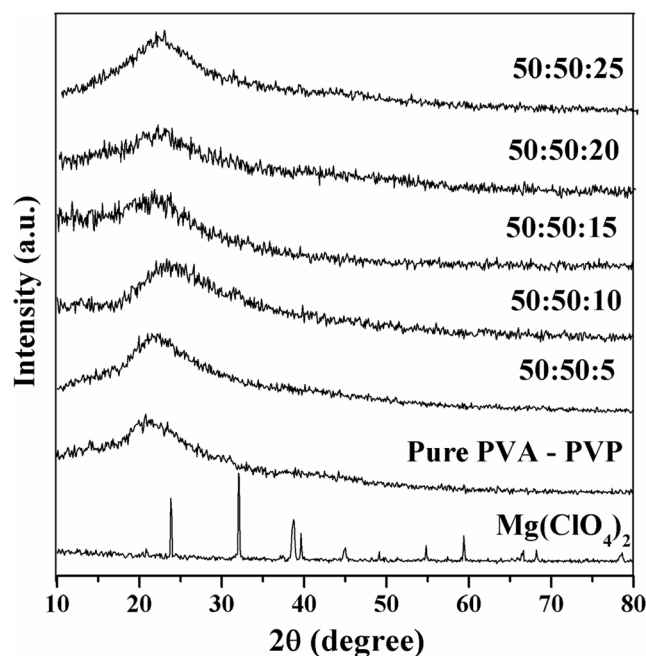


Fig. 2 XRD pattern of $\text{Mg}(\text{ClO}_4)_2$, pure PVA–PVP blend and PVA–PVP BPEs with different concentration of $\text{Mg}(\text{ClO}_4)_2$

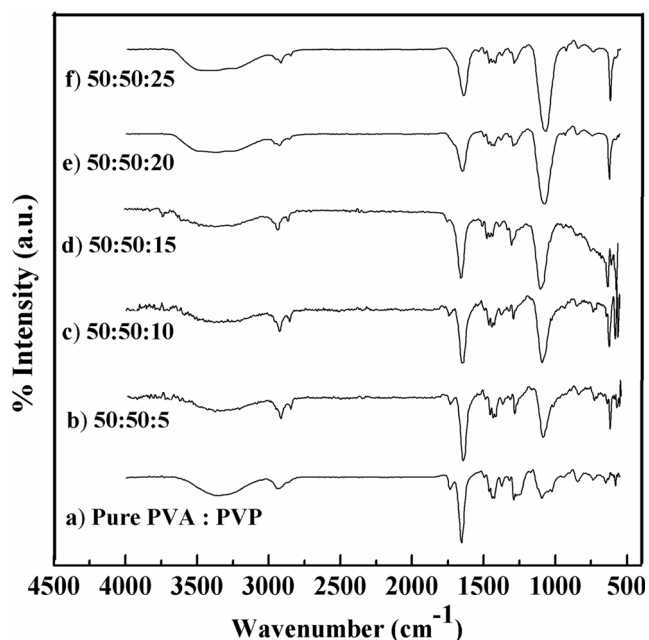


Fig. 3 FTIR spectra of pure PVA–PVP blend and PVA–PVP BPE with different concentrations of $\text{Mg}(\text{ClO}_4)_2$

shifted to lower wave number side upon incorporation of $\text{Mg}(\text{ClO}_4)_2$. The decrease in the intensity of the peak and its shifting towards lower wave number side indicates the formation of ion dipole $\text{C}=\text{O} \cdots \cdots \text{Mg}^{2+}$ complex [26]. The peaks at $1091\text{--}1069\text{ cm}^{-1}$ are resulted from the C–O stretching of the residual acetate groups present in PVA (due to the manufacture of PVA from hydrolysis of polyvinyl acetate). With increase in salt concentration, the band appearing at 1091 cm^{-1} in the pure PVA–PVP blend gets shifted to lower wave numbers and a decrease in its intensity is observed. The change in the band position is a consequence of ion–dipole interactions, which change the local electronic structure of the chain. The changes observed for C–O vibrational band indicate the flexibility of the polymer chains. Similar reports were reported in literature for PVA-based polymer electrolytes [27]. The appearance of a new peak at 622 cm^{-1} in the salt-doped polymer blends is assigned to the symmetrical stretching of perchlorate anion. This peak is very sensitive to ion association, i.e. the perchlorate ion is expected to reassociate with cation of the dopant at higher salt concentration. This leads to the change in the frequency position of the peak observed around 622 cm^{-1} . In the present case, peak position remains unchanged with increasing salt concentration which excludes the possibility of ion association [28]. The appearance of new peak along with changes in existing peaks in the FTIR spectra is a direct indication of the complexation of PVA–PVP with $\text{Mg}(\text{ClO}_4)_2$.

DSC analysis

DSC analysis has been employed to observe the changes in glass transition (T_g) and melting temperature (T_m) that is

caused by the blending of two polymers and addition of the dopant. All the BPEs show a single T_g between 73 and $88\text{ }^\circ\text{C}$ indicating the compatibility of the polymers (Fig. 4(a)) [29, 30]. The observed T_g value increases with increase in dopant concentration indicate the stiffening of the polymer chains due to the interaction of the cation with the electronegative centres of the polymer backbone. The elevation of T_g could be correlated to the number of free ‘Mg’ ions—more is the number of free charge carriers, higher is the elevation of T_g . This behaviour is presumed that T_g will increase owing to the formation of transient cross-linking knots formed between the free ions ($\text{Mg}^{2+}/\text{ClO}_4^{2-}$) and hydroxyl group/pyrrolidone group of PVA/PVP, respectively [31, 32]. Here, in this situation, the cations/anions will have more than one coordination site to interact and serve as cross-linking agent for the polymer. The most favourable inter-chain interactions in a PVA–PVP system in the presence and absence of the dopant are shown in Scheme 1.

By further analysing the thermograms (Fig. 4(b)), the pure PVA–PVP blend shows a single broad endothermic peak around $143\text{ }^\circ\text{C}$. The presence of single melting peak indicates the miscibility of both the polymers. Upon addition of dopant to the polymer blend during the preparation stage resulted in the formation of polymer–salt complexes and a change in the crystallization nature of the sample. The shift in T_m towards higher temperatures for all the blend polymer electrolytes indicates the improved thermal stability of the BPEs. Closer inspection of the thermogram for 15 m% of the salt-doped BPE shows a sharp endothermic peak at $195\text{ }^\circ\text{C}$ and a small endothermic peak at $157\text{ }^\circ\text{C}$. The peak at $157\text{ }^\circ\text{C}$ becomes more prominent when the dopant concentration is increased to 20 and 25 m% $\text{Mg}(\text{ClO}_4)_2$. The above results suggest the formation of polymer–salt complexes. Further, the splitting of the melting endotherm at higher dopant concentration may be attributed to any of the following reasons (i) presence of pure PVA–PVP phase, (ii) PVA–PVP– $\text{Mg}(\text{ClO}_4)_2$ complex phase and (iii) multiple states of the salts, i.e. salt aggregates, partially solvated and completely complexed dopant within the polymer [33, 34].

A.C. impedance analysis

The complex impedance plot (Z' vs Z'') (Fig. 5) for the BPEs at 303 K shows two well-defined regions, i.e. (i) the semicircular portion at high-frequency region arises from a parallel combination of the bulk resistance of the cell and (ii) the linear region with slight curvature in the low-frequency side is due to the effect of blocking electrodes [35]. In the impedance set-up, the two stainless steel plates act as blocking electrodes, and the electrolyte interface can be regarded as the capacitor [36]. If the capacitor is ideal, it should give rise to a vertical spike parallel to the y -axis in the impedance plot. The observed spikes in the plot are non-vertical in nature and they are

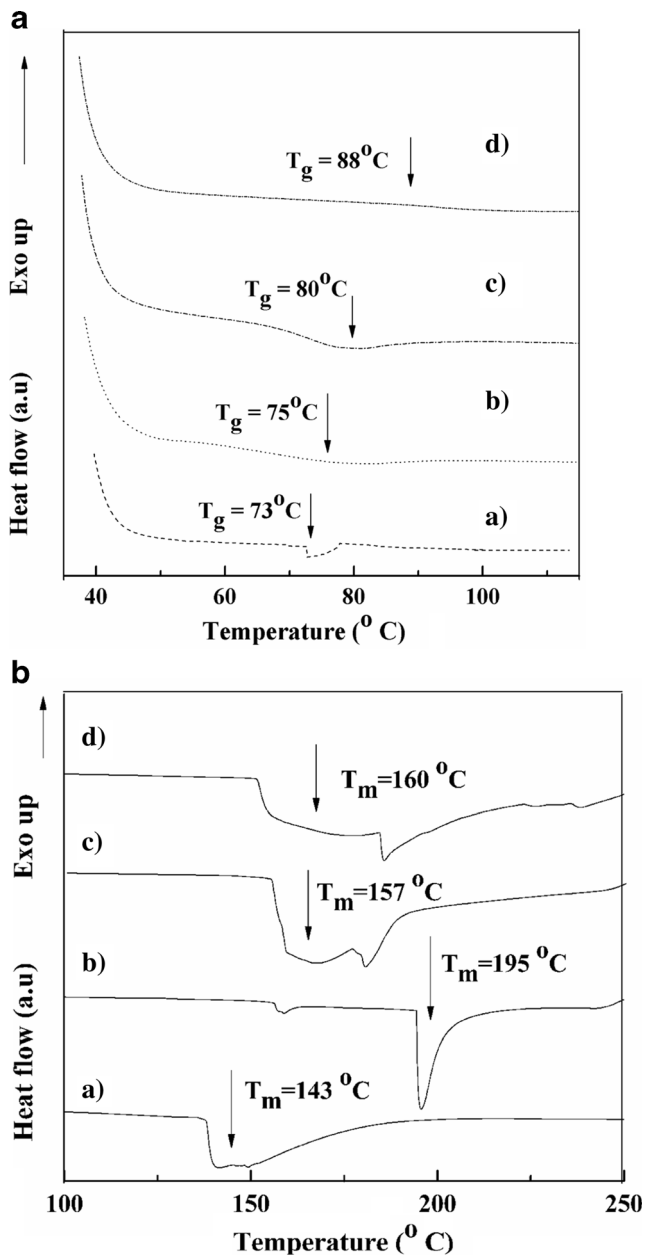


Fig. 4 DSC thermogram **a** glass transition temperature (T_g) and **b** melting temperature (T_m) of pure PVA–PVP (*a*), 50:50:15 (*b*), 50:50:20 (*c*) and 50:50:25 (*d*)

inclined at an angle less than 90° , indicating the non-ideal mode of capacitance behaviour in the polymer electrolytes and thus lead to the configuration of electrical double layer at electrolyte and electrode interface [37]. The observed semicircles are found to be depressed below the real axis and the angle by which the semicircle is depressed below the real axis and the amount of inclination in the spike is related to the width of the relaxation time distribution. These results suggest the presence of constant phase element at the electrode–electrolyte interface and the non-Debye nature of the samples [38, 39]. The bulk resistance (R_b) of the polymer electrolytes is

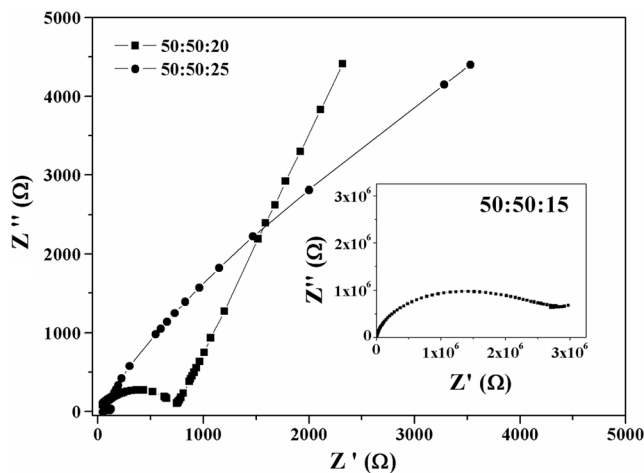


Fig. 5 Cole–Cole plot for the BPEs with different concentrations of $Mg(ClO_4)_2$ at RT

calculated from the intercept of the high-frequency semicircle or low-frequency spike on the real impedance (Z') axis. By knowing the value of bulk resistance along with the dimensions of the sample, the conductivity has been calculated for all compositions using the relation,

$$\sigma = L/R_b A \tag{1}$$

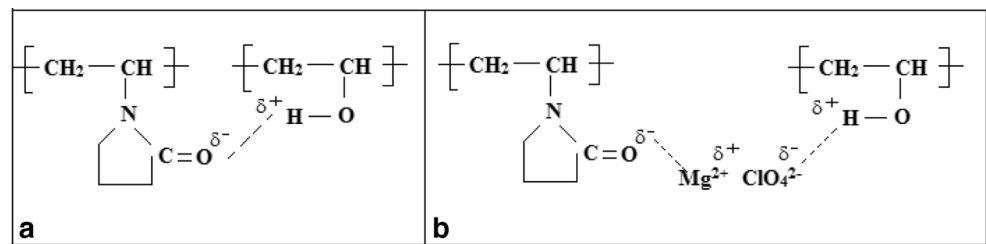
where L and A are the thickness and the area of the samples, respectively. It is apparent from Fig. 5 that the diameter of the semicircle gradually decreases with the addition of the dopant. The semicircular portion is characteristic of parallel combination of bulk resistance and bulk capacitance. The decrease in the diameter of the semicircular portion at higher frequency is due to the random dipole orientation of the polar side groups present in the polymer network owing to the non-capacitive nature. Therefore, only the resistive components in the polymer electrolytes prevail which constructs a conducting pathway for the ions to move in the polymer matrix. The value of conductivity calculated using Eq. (1) for all compositions at room temperature is listed in Table 1. The highest ionic conductivity at room temperature has been obtained as $1.1 \times 10^{-4} \text{ S cm}^{-1}$ for the BPE with 25 mol% $Mg(ClO_4)_2$.

Conductivity is related to the number of charge carriers (n) and their mobility (μ) according to the following equation:

$$\sigma = n \cdot q \cdot \mu \tag{2}$$

where q is the charge on each charge carrier. The effect of adding $Mg(ClO_4)_2$ shows a pronounced effect on the conductivity of the PVA–PVP blend polymer electrolyte. This observed increase in ionic conductivity with increasing dopant concentration can be explained on the basis of breathing chain model. According to the model, the opening and folding of the polymeric chains are associated with a free volume change [40]. This microscopic fluctuation may lead to the dissociation

Scheme 1 **a** Inter-chain interaction of PVA–PVP in the absence of dopant. **b** Inter-chain interaction of PVA–PVP in the presence of dopant



of the dopant resulting in the increase in the number of mobile charge carriers and mobility.

Figure 6 shows temperature dependence of ionic conductivity of BPEs in the temperature range 303 to 343 K. The highest conducting sample, 50:50:25, has an ionic conductivity of $1.1 \times 10^{-4} \text{ S cm}^{-1}$ at room temperature and $1.2 \times 10^{-3} \text{ S cm}^{-1}$ at 343 K. This opens a new window for the use of magnesium-based batteries in practical applications over a wide range of temperatures. The ionic conductivity exhibits linear dependence with temperature (within the temperature range studied), which indicates Arrhenius-type thermally activated process for the ion conduction in the BPEs. The polymer complexes do not show any abrupt jump with temperature which indicates the increase in amorphicity of the BPEs [41]. As the amorphous region increases, the polymer chain acquires faster internal modes in which bond rotations produce segmental motion which in turn favours inter- and intra-chain ion hopping, and thus, the degree of conductivity becomes high [42]. The activation energy (E_a) for the BPEs has been obtained by the linear fitting of the Arrhenius equation,

$$\sigma = (\sigma_o/T)\exp(-E_a/KT) \quad (3)$$

where σ_o is the pre-exponential factor and K is the Boltzmann constant. As expected, the highest conducting sample possesses the lowest activation energy. Activation energy is often found to be higher in magnesium-based polymer electrolytes, as compared to their lithium counterpart [43]. This can be thought to

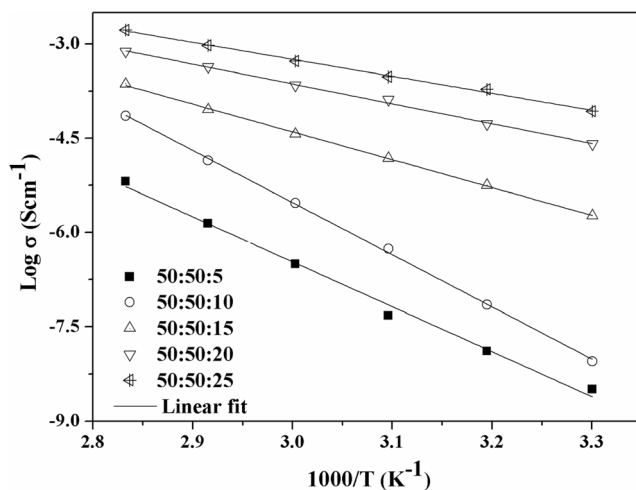


Fig. 6 $\text{Log } \sigma$ vs $1000/T$ plot for polymer electrolytes with different concentrations of $\text{Mg}(\text{ClO}_4)_2$

be due to either the greater interaction between the metal ions and the solvent molecules and/or the formation of multiple ions, which restricts their movement [44]. The activation energy (E_a) and the regression values (R) of the BPEs have been tabulated in Table 1.

Dielectric analysis

The frequency dependence of dielectric constant as a function of frequency for blend polymer electrolytes is shown in Fig. 7. At low frequencies, the dielectric constant is maximum and it becomes almost frequency independent at higher frequencies. At low frequencies, the charge carriers have enough time to build up at the electrode–electrolyte interface leading to the localization of charge carriers. Thus, the electrode polarization effects contribute to the high value of dielectric constant at low frequency. As the frequency increases, the charge carriers that were oscillating along the direction of the field will now lag behind, resulting in low value of dielectric constant [45]. As the dielectric constant is the direct measure of the charges stored in a material, the high dielectric constant obtained for 20 and 25 mol% of $\text{Mg}(\text{ClO}_4)_2$ BPE is an evidence of the increase in the density of ions and hence increased conductivity [46].

The amount of energy dissipated is reflected by the presence of loss peak in the dielectric loss spectra. The dielectric loss spectra for the BPE with 25 mol% $\text{Mg}(\text{ClO}_4)_2$ at various

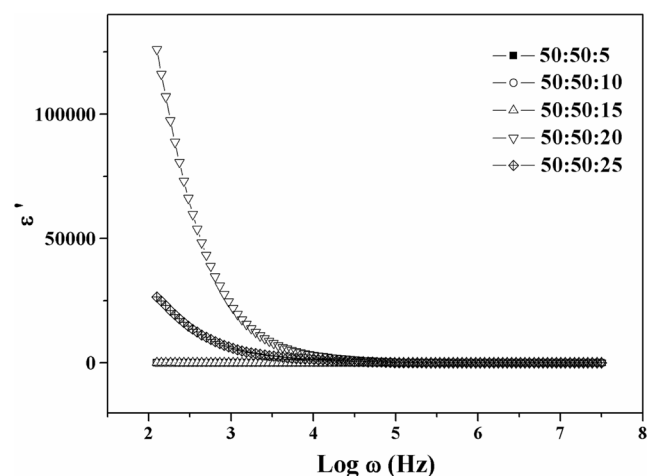


Fig. 7 Plot of $\text{log } \epsilon'$ vs. $\text{log } f$ for BPEs with different concentrations of $\text{Mg}(\text{ClO}_4)_2$ at RT

temperatures is shown in Fig. 8. From the plot, the peak observed at high frequencies is due to β -relaxation and this relaxation processes may be caused by movement of the side chains. The presence of β -peak in the dielectric loss spectra is a proof for the diffusion of ions accompanied by the polymer segmental mobility [47]. The frequency at which the peak maxima occurs shifts towards higher frequency region with increase in temperature, evidences the coordination/de-coordination of Mg^{2+} ions with the polymer backbone. Here, the segmental motion facilitates charge migration between PVA/PVP chains. Similar reports are available in literature for PEG- δ - $MgCl_2$ -based polymer electrolytes [48].

Dopant concentration-dependent modulus analysis

The electric modulus spectrum is a useful tool to investigate the conductivity and its associated relaxation in polymer electrolytes. The plot between $\log \omega$ and M' (Fig. 9) confirms almost zero M' values at low frequencies corresponding to the suppression of electrode polarization effects [49]. As the frequency increases, the M' value also increases and reaches to maximum value at higher frequencies for all dopant concentration that suggest the distribution of relaxation process over a range of frequencies. A long tail in the low-frequency side is observed in the plot for 20 and 25 m% $Mg(ClO_4)_2$ -doped BPE that indicates the large capacitance value associated with the electrode polarization effects [50, 51]. Also, the reduction in the M' value with increasing $Mg(ClO_4)_2$ concentration represents the increased carrier density and the polymer segmental mobility.

Well-defined peaks are observed in the $\log \omega$ vs M'' spectra as shown in Fig. 10. The peaks are broader and asymmetric on both the sides of the maxima than predicted by ideal Debye behaviour. The frequency range where the peak occurs is an indicative of transition from long range to short range

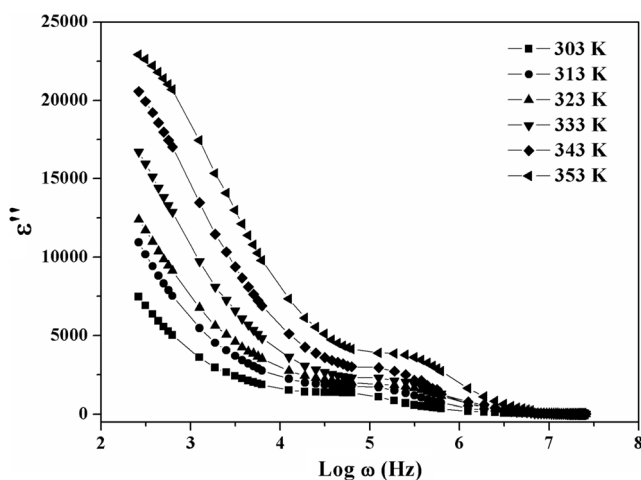


Fig. 8 Plot of $\log \epsilon''$ vs. $\log f$ for BPE with 25 m% $Mg(ClO_4)_2$ at various temperatures

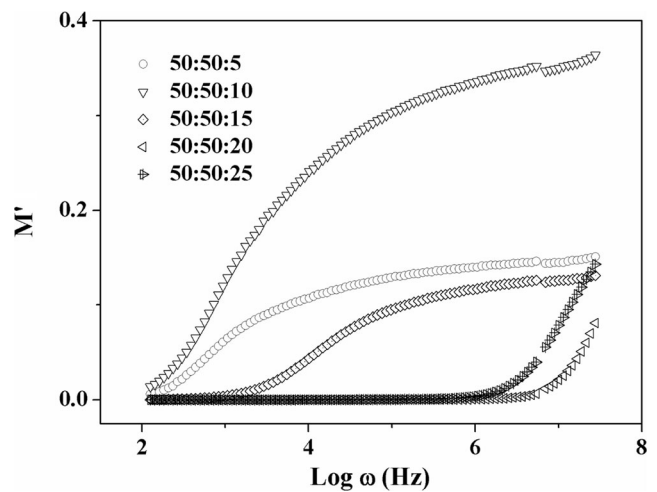


Fig. 9 Variation of real part of modulus (M') with frequency for BPEs with different concentrations of $Mg(ClO_4)_2$ at RT

mobility. The peak in the low-frequency region represents the movement of ions over long distances, whereas the high-frequency peak represents the short range movement of the ions [52]. From the plot, it is apparent that the peak position shifts to higher frequency and there is a decrease in the height of the peak as the dopant concentration increases suggesting the fast relaxation of the ions. The asymmetric M'' plot represents the distribution of relaxation time and non-Debye nature of the blend polymer electrolytes. To confirm the non-Debye nature of the relaxation in the BPEs, an Argand plot has been drawn for all the compositions and it is shown in Fig. 11. A complete semicircle in the Argand plot represents the Debye-type relaxation in the polymer electrolytes. In the present case, the Argand plots are markedly non-semicircular in nature indicating the relaxation is of non-Debye type having multiple relaxation times [53]. The reason for the distribution of relaxation times may be due to the presence of polar groups, space charge polarization and in-homogeneities in the polymer

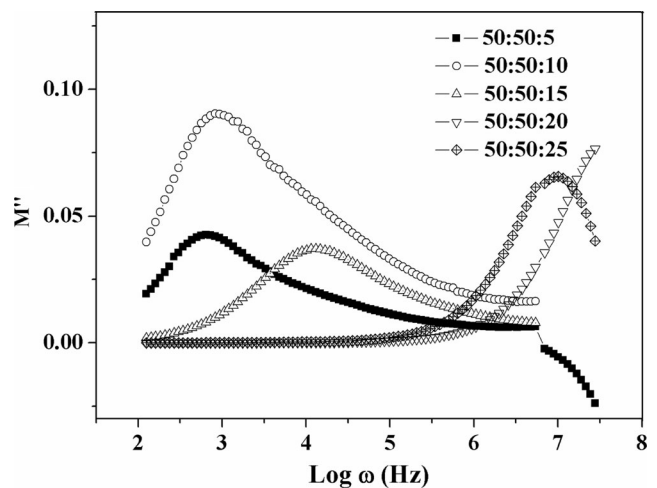


Fig. 10 Variation of imaginary part of modulus (M'') with frequency for BPEs with different concentrations of $Mg(ClO_4)_2$ at RT

electrolytes. It is seen from Fig. 11 that, with increasing dopant concentration, the Argand curves shift towards the origin which may be ascribed to the increase of conductivity with increase in dopant concentration.

Transference number measurements

The total transport number gives a quantitative evaluation of the extent of ionic and electronic contributions to the total conductivity. To determine the nature of species responsible for the conductivity in the present electrolyte system, the total ionic transference number was found by applying a small D.C. potential of 0.7 V across SS/BPE/SS cell configuration at room temperature. The inset in Fig. 12 (b (i)) shows the current vs time plot for the blend polymer electrolyte with 25 m% $\text{Mg}(\text{ClO}_4)_2$. The value of t_{ion} was determined by using the following equation,

$$t_{\text{ion}} = 1 - (i_e / i_T) \quad (4)$$

where i_T is the total current and i_e is the residual current. The total ionic transference number was found to be >0.95 for all the BPEs which indicates the charge carriers are ions. In the present system, both cations (Mg^{2+}) and anions (ClO_4^{2-}) being the mobile charge carriers, it is essential to find the transference number of the Mg^{2+} ions to the total conductivity. The Mg^{2+} transport number for the BPEs was evaluated using A.C./D.C. techniques, proposed by Evans et al. [54]. In this technique, the symmetrical cell $\text{Mg}/\text{BPE}/\text{Mg}$ was polarized by a small D.C. voltage of 0.5 V and the initial and the final current values were obtained from the current-time plot as shown as an inset in Fig. 12 (b (ii)). The cell resistances before and after polarization (after the cell reaches steady-state) were obtained from impedance measurements. It is evident from the impedance plot (Fig. 12 (a)) that the bulk resistance (R_b) of the cell does not change before and after polarization suggesting

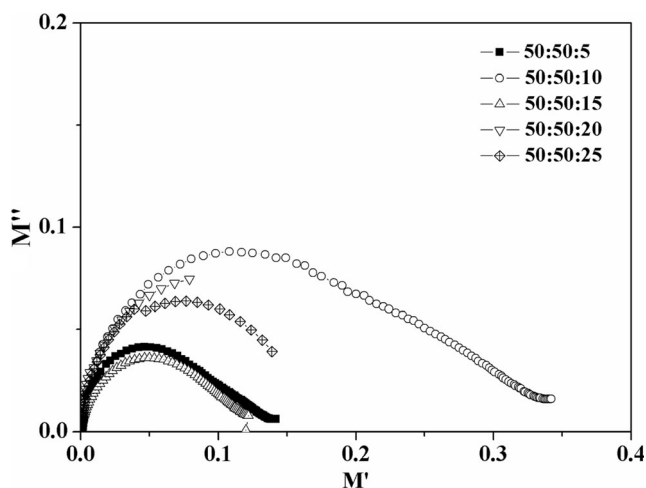


Fig. 11 Argand plot for BPEs with different concentrations of $\text{Mg}(\text{ClO}_4)_2$ at RT

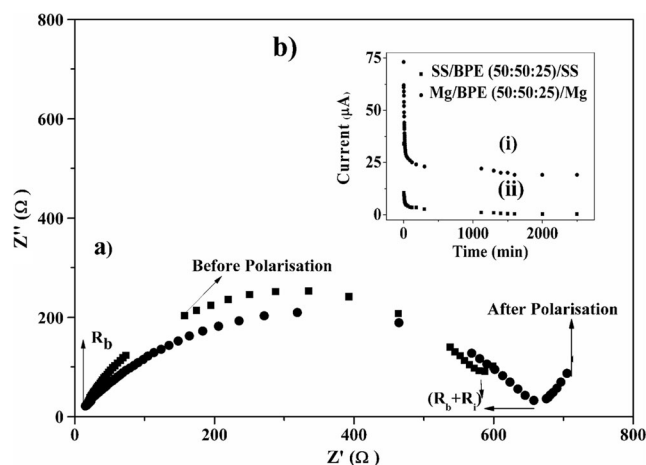


Fig. 12 A.C. complex impedance plot before and after polarization of a typical symmetric $\text{Mg}/50\text{PVA}:50\text{PVP}:25 \text{Mg}(\text{ClO}_4)_2/\text{Mg}$ cell (a). Inset showing the D.C. polarization curve of $\text{SS}/50\text{PVA}:50\text{PVP}:25 \text{Mg}(\text{ClO}_4)_2/\text{SS}$ cell (i) and $\text{Mg}/50\text{PVA}:50\text{PVP}:25 \text{Mg}(\text{ClO}_4)_2/\text{Mg}$ cell at room temperature (ii) (b)

that the composition of the BPE did not change even after polarization. But the diameter of the semicircle at the low-frequency region, which is due to the total impedance ($R_b + R_i$ (R_i is the resistance of the passivating layer)) of the cell, has increased signifying the formation of passivating layer. Osman et al., Kumar et al. and Pandey et al. have obtained similar results for PMMA- and PEO-based polymer electrolytes respectively [55–57]. The values of Mg^{2+} transport number were calculated using the formula,

$$t_+ = I_s (\Delta V - R_o I_o) / I_o (\Delta V - R_s I_s) \quad (5)$$

where I_o and I_s are the initial and the final current, respectively. R_o and R_s are the cell resistance before and after polarization, respectively. The value of $t_{\text{Mg}^{2+}}$ found using Eq. (5) is given in Table 1.

Linear sweep voltammetry and cyclic voltammogram studies

The electrochemical stability is an important characteristic of a polymer electrolyte for its technological application, and it has been examined by linear sweep voltammetry. The LSV was performed for the optimum conducting BPE (50 PVA/50 PVP/25 $\text{Mg}(\text{ClO}_4)_2$) and is shown in Fig. 13. The LSV was recorded on SS/BPE/Mg at a scan rate of 5 mV s^{-1} . The sudden rise in the current observed from the plot is due to the decomposition of the electrolyte at the blocking electrode. It is found that the BPE is stable up to 3.5 V [58]. The electrochemical stability found seems to be convenient for its application in magnesium ion batteries.

The investigation of electrochemical reversibility of Mg/Mg^{2+} from a blend polymer electrolyte is essential for its potential application in magnesium batteries. The CV

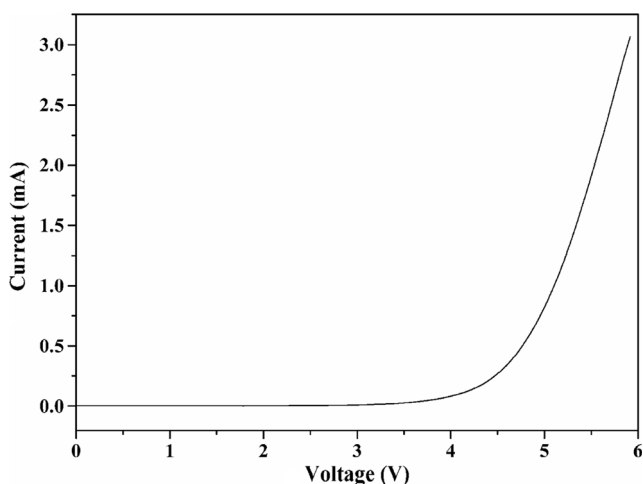


Fig. 13 Linear sweep voltammometry of SS/BPE(50:50:25)/Mg cell recorded at a scan rate of 5 mV s^{-1} at room temperature

measurements have been carried out on the following two symmetrical cells using BPE with 25 mol% $\text{Mg}(\text{ClO}_4)_2$.

Cell 1: SS/50 PVA/50 PVP/25 mol% $\text{Mg}(\text{ClO}_4)_2$ /SS

Cell 2: Mg/50 PVA/50 PVP/25 mol% $\text{Mg}(\text{ClO}_4)_2$ /Mg

Figure 14 shows the comparative CV plots of cell 1 and cell 2 taken at a scanning rate of 5 mV s^{-1} . The voltammogram shows two distinct cathodic and anodic current peaks for cell 2, whereas no such features are observed for cell 1 in the same potential range. This suggests that the cathodic deposition and anodic oxidation of Mg are facile at the Mg electrode and the BPE interface due to the following reversible reaction.



The peak potential separation is several volts apart, which is the effect of two electrode geometry with no reference

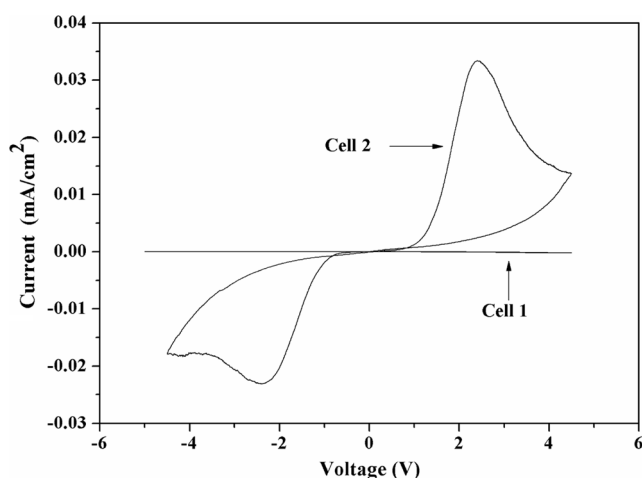


Fig. 14 Cyclic voltammogram of (SS)Mg/50:50:25 BPE/Mg(SS) symmetrical cells at a scan rate of 5 mV s^{-1} at room temperature

electrode. However, on the anodic side, the current profile should be the superposition of the currents arising from (a) the Mg oxidation and (b) the decomposition of the electrolytes. But, at potential higher than the stripping peak maximum, the current does not reach zero value, indicating that decomposition of the electrolyte started at a lower voltage. Such studies are reported in similar systems in the literature [56, 58–60].

Conclusion

Solid electrolytes based on PVA–PVP blend with and $\text{Mg}(\text{ClO}_4)_2$ have been prepared by solution casting method. The XRD results reveal that the increased amorphous content in the polymer electrolytes leads to conductivity value reaching $10^{-4} \text{ S cm}^{-1}$ in the absence of humidity. The conductivity enhancement in the present system is the direct consequence of the inter-/intra-molecular interactions between the PVA and PVP, which creates conduction pathway for the free charge carriers to move. The thermal studies reveal that a single glass transition for all the dopant concentration indicates the miscibility of the polymers. Also, the magnesium ions play the role of transient cross-link centres, enhancing the miscibility and the thermal stability of the polymer electrolytes. The measured dielectric data in terms of dielectric spectra and electric modulus confirms the electrode polarization, polymer segmental motion, conductivity relaxation and the distribution of the relaxation times in the BPEs. The transport number study confirms the Mg^{2+} ion conduction in the BPEs. The electrochemical stability window, estimated from LSV, is found to be $\sim 3.5 \text{ V}$, which is sufficient for electrochemical applications. The cyclic voltammetry suggests the existence of electrochemical equilibrium between the Mg metal and Mg^{2+} ions in the blend polymer electrolyte.

Acknowledgements One of the authors Mrs. Mangalam Ramaswamy would like to thank the Principal and Management, PSG Institute of Technology and Applied Research for the support extended towards this research work. A special thanks is addressed to Dr. S. Harish and Dr. A. Kumaravel, Department of Chemistry, PSG Institute of Technology and Applied Research, for their comments that improved the LSV and CV studies.

References

1. Yoo HD, Shterenberg I, Gofer Y, Gershinshy G, Pour N, Aurbach D (2013) Mg rechargeable batteries: an on-going challenge. *Energy Environ Sci* 6:2265–2279
2. Song J, Sahadeo E, Noked M, Lee SB (2016) Mapping the challenges of magnesium battery. *J Phys Chem Lett* 7:1736–1749
3. Bertasi F, Vezzù K, Nawn G, Pagot G, Di Noto V (2016) Interplay between structure and conductivity in 1-ethyl-3-methylimidazolium tetrafluoroborate/ $(\delta\text{-MgCl}_2)$ f electrolytes for magnesium batteries. *Electrochim Acta* 219:152–162

4. Bertasi F, Hettige C, Sepehr F, Bogle X, Pagot G, Vezzù K, Negro E, Paddison SJ, Greenbaum SG, Vittadello M, Di Noto V (2015) A key concept in magnesium secondary battery electrolytes. *ChemSusChem* 18:3069–3076
5. Tang X, Muchakayala R, Song S, Zhang Z, Polu AR (2016) A study of structural, electrical and electrochemical properties of PVdF-HFP gel polymer electrolyte films for magnesium ion battery applications. *J Ind Eng Chem* 37:67–74
6. Sheha EM, Nasr MM, El-Mansy MK (2015) The role of MgBr₂ to enhance the ionic conductivity of PVA/PEDOT:PSS polymer composite. *J Adv Res* 6:563–569
7. Bannister DJ, Davis GR, Ward IM, Melntyre JE (1984) Ionic conductivities for poly(ethylene oxide) complexes with lithium salts of monobasic and dibasic acids and blends of poly(ethylene oxide) with lithium salts of anionic polymers. *Polymer* 25:1291–1296
8. Wieczorek W, Florjanczyk Z, Stevens JR (1995) Proton conducting polymer gels based on a polyacrylamide matrix. *Electrochim Acta* 40:2327–2330
9. Prajapathi GK, Roshan R, Gupta PN (2010) Effect of plasticizer on ionic transport and dielectric properties of PVA:H₃PO₄ proton conducting polymeric electrolytes. *J Phys Chem Solids* 71:1717–1723
10. Shammukaraj D, Wang GX, Murugan R, Liu HK (2008) Ionic conductivity and electrochemical stability of poly (methylmethacrylate)–poly (ethylene oxide) blend-ceramic fillers composites. *J Phys Chem Solids* 69:243–248
11. Abdelrazek EM, Elashmawi IS, El-khodary A, Yassin A (2010) Structural, optical, thermal and electrical studies on PVA/PVP blends filled with lithium bromide. *Curr Appl Phys* 10:607–613
12. Rajeswari N, Selvasekarapandian S, Prabhu M, Karthikeyan S, Sanjeeviraja C (2013) Lithium ion conducting solid polymer blend electrolyte based on bio-degradable polymers. *Bull Mater Sci* 36: 333–339
13. Rajeswari N, Selvasekarapandian S, Karthikeyan S, Sanjeeviraja C, Iwai Y, Kawamura J (2013) Structural, vibrational, thermal, and electrical properties of PVA/PVP biodegradable polymer blend electrolyte with CH₃COONH₄. *Ionics* 19:1105–1113
14. Kulshrestha N, Gupta PN (2016) Structural and electrical characterizations of 50:50 PVA:starch blend complexed with ammonium thiocyanate. *Ionics* 22:671–681
15. Sivadevi S, Selvasekarapandian S, Karthikeyan S, Sanjeeviraja C, Nithya H, Iwai Y, Kawamura J (2015) Proton-conducting polymer electrolyte based on PVA-PAN blend doped with ammonium thiocyanate. *Ionics* 21:1017–1029
16. Rathika R, Austin Suthanthiraraj S (2016) Ionic interactions and dielectric relaxation of PEO/PVdF-Mg[(CF₃SO₂)₂N₂] blend electrolytes for magnesium ion rechargeable batteries. *Macromol Res* 24:422–428
17. Polu AR, Kumar R, Rhee H-W (2015) Magnesium ion conducting solid polymer blend electrolyte based on biodegradable polymers and application in solid-state batteries. *Ionics* 21:125–132
18. Hefford RJ (1984) Polymer mixing in aqueous solution. *Polymer* 25:979–984
19. Yoshiyuki N, Haratami T, Takahashi T (1990) Miscibility and orientation behavior of poly(vinyl alcohol)/poly(vinyl pyrrolidone) blends. *J Polym Sci B Polym Phys* 28:355–376
20. Lewandowska K (2005) The miscibility of poly(vinyl alcohol)/poly(N-vinylpyrrolidone) blends investigated in dilute solutions and solids. *Eur Polym J* 41:55–64
21. Rajendran S, Sivakumar M, Subadevi R (2004) Investigations on the effect of various plasticizers in PVA–PMMA solid polymer blend electrolytes. *Mater Lett* 58:641–649
22. Choudhary S, Sengwa RJ (2013) Effects of preparation methods on structure, ionic conductivity and dielectric relaxation of solid polymeric electrolytes. *Mater Chem Phys* 142:172–181
23. Karmakar A, Gosh A (2012) Dielectric permittivity and electric modulus of polyethylene oxide (PEO)–LiClO₄ composite electrolytes. *Curr Appl Phys* 12:539–543
24. Sengwa RJ, Choudhary S (2014) Dielectric properties and fluctuating relaxation processes of poly(methyl methacrylate) based polymeric nanocomposite electrolytes. *J Phys Chem Solids* 75:765–774
25. Kumar A, Logapperumal S, Sharma R, Das MK, Kar KK (2016) Li-ion transport, structural and thermal studies on lithium triflate and barium titanate incorporated poly(vinylidene fluoride-co-hexafluoropropene) based polymer electrolyte. *Soild State Ionics* 289:150–158
26. Rocco AM, Pereira RP (2015) Solid electrolytes based on poly (ethylene oxide)/poly(4-vinyl phenol-co-2-hydroxyethyl methacrylate blends and LiClO₄). *Solid State Ionics* 279:78–89
27. Rajendran S, Sivakumar M, Subadevi R (2004) Li-ion conduction of plasticized PVA solid polymer electrolytes complexed with various lithium salts. *Solid State Ionics* 167:335–339
28. Jaipal Reddy M, Chu PP (2002) Effect of Mg²⁺ on PEO morphology and conductivity. *J Power Sources* 109:340–346
29. Baskaran R, Selvasekarapandian S, Kuwata N, Kawamura J, Hattori T (2006) AC impedance, DSC and FT-IR investigations on (x) PVAc–(1– x) PVdF blends with LiClO₄. *Mater Chem Phys* 98:55–61
30. Francis KMG, Subramanian S, Shunmugavel K, Naranappa V, Pandian SSM, Nadar SC (2016) Lithium ion-conducting blend polymer electrolyte based on PVA–PAN doped with lithium nitrate. *Polym-Plast Technol Eng* 55:25–35
31. Brail D, Michot C, Armand M (1997) Electrochemistry of liquids vs. solids: polymer electrolytes. *Solid State Ionics* 94:35–47
32. Cassu SN, Felisberti MI (1997) Dynamic mechanical behavior and relaxations in polymers and polymeric blends. *Polymer* 38:3907–3911
33. Agrawal SL, Rai N, Chand N (2013) Dynamic mechanical, DSC, and electrical investigations on Nano Al₂O₃ filled PVA:NH₄SCN:DMSO polymer composite dried gel electrolytes. *Int J Polym Mater* 62:61–67
34. Arvind A, Agarwal SL (2007) Structural, thermal and electrical characterizations of PVA:DMSO:NH₄SCN gel electrolytes. *Solid State Ionics* 178:961–958
35. Prajapati GK, Gupta PN (2011) Comparative study of the electrical and dielectric properties of complex polymer electrolytes. *Physica B* 406:3108–3113
36. MacCallum JR, Vincent CA (1987) Polymer electrolyte reviews, vol 1. Elsevier Applied Science Edition, London Chapters 1 and 8
37. Renganathan NG, Kumar TP, Thirunakaran R, Pitchumani S, Shrisudersan J, Muniyandi N (2000) Ionic conductivity studies on plasticized PVC/PMMA blend polymer electrolyte containing LiBF₄ and LiCF₃SO₃. *Solid State Ionics* 130:123–132
38. Wu GM, Lin SJ, Yang CC (2006) Preparation and characterization of PVA/PAA membranes for solid polymer electrolytes. *J Membr Sci* 275:127–133
39. Macdonald JR (ed) (1987) Impedance spectroscopy. Wiley, New York
40. Chandra S, Sekhon SS, Arora N (2000) PMMA based protonic polymer gel electrolytes. *Ionics* 6:112–118
41. Ramesh S, Chai MF (2007) Conductivity, dielectric behavior and FTIR studies of high molecular weight poly(vinylchloride)–lithium triflate polymer electrolytes. *Mater Sci Eng B* 139:240–245
42. Shukla N, Thakur AK (2009) Role of salt concentration on conductivity optimization and structural phase separation in a solid polymer electrolyte based on PMMA–LiClO₄. *Ionics* 15:357–367
43. Lee KY, Chung WS, Jo NJ (2004) Effect of salt species on electrochemical properties of gel-type polymer electrolyte based on chemically crosslink rubber. *ElectrochimActa* 50:295–300
44. Ikeda S, Mori Y, Furuhashi Y, Masuda H (1999) Multivalent cation conductive solid polymer electrolytes using photo-cross-linked polymers. II. Magnesium and zinc trifluoromethanesulfonate systems. *Solid State Ionics* 21:329–333

45. Subba Reddy CV, Han X, Zhu Q-Y, Mai L-Q, Chen W (2006) Dielectric spectroscopy studies on (PVP + PVA) polyblend film. *Microelectron Eng* 83:281–285
46. Sengwa RJ, Dhatarwal P, Choudhary S (2015) Effects of plasticizer and nanofiller on the dielectric dispersion and relaxation behaviour of polymer blend based solid polymer electrolytes. *Curr Appl Phys* 15:135–143
47. Nithya H, Selvasekarapandian S, Arunkumar D, Christopherselvan P, Kawamura J, Baskaran R, Sanjeeviraja C (2011) Thermal and dielectric studies of polymer electrolyte based on P(ECH-EO). *Mater Chem Phys* 126:404–408
48. Piccolo M, Giffin GA, Vezz K, Bertasi F, Alotto P, Guarnieri M, Di Noto V (2013) Molecular relaxations in magnesium polymer electrolytes via GHz broadband electrical spectroscopy. *ChemSusChem* 6:2157–2160
49. Cheruku R, Vijayan L, Govindaraj G (2012) Electrical relaxation studies of solution combustion synthesized nanocrystalline $\text{Li}_2\text{NiZrO}_4$ material. *Mater Sci Eng B* 177:771–779
50. Fadzallah A, Majid SR, Careem MA, Arof AK (2014) Relaxation process in chitosan–oxalic acid solid polymer electrolytes. *Ionics* 20:969–975
51. Aziz SB, Abidin ZHZ, Arof AK (2010) Influence of silver ion reduction on electrical modulus parameters of solid polymer electrolyte based on chitosan-silver triflate electrolyte membrane. *Express Polym Lett* 4:300–310
52. Woo HJ, Majid SR, Arof AK (2012) Dielectric properties and morphology of polymer electrolyte based on poly (ϵ -caprolactone) and ammonium thiocyanate. *Mater Chem Phys* 134:755–761
53. Kwan KC (2004) *Dielectric phenomena in solids*. Elsevier, NewYork
54. Evans J, Vincent CA, Bruce PG (1988) Electrochemical measurement of transference numbers in polymer electrolytes. *Polymer* 28: 2324–2328
55. Osman Z, Zainol NH, Samin SM, Chong WG, Md Isa KB, Othman L, Supa'at I, Sonsudin F (2014) Electrochemical impedance spectroscopy studies of magnesium-based polymethylmethacrylate gel polymer electrolytes. *Electrochim Acta* 131:148–153
56. Girish Kumar G, Munichandraiah N (2002) Polymethylmethacrylate–magnesium triflate gel polymer electrolyte for solid state magnesium battery application. *Electrochim Acta* 47:1013–1022
57. Pandey GP, Agrawal RC, Hashmi SA (2011) Magnesium ion-conducting gel polymer electrolytes dispersed with fumed silica for rechargeable magnesium battery application. *J Solid State Electrochem* 15:2253–2264
58. Sharma J, Hashmi SA (2013) Magnesium ion transport in poly(ethylene oxide)-based polymer electrolyte containing plastic-crystalline succinonitrile. *J Solid State Electrochem* 17:2283–2291
59. Yogesh K, Hashmi SA, Pandey GP (2011) Ionic liquid mediated magnesium ion conduction in poly (ethylene oxide) based polymer electrolyte. *Electrochim Acta* 56:3864–3873
60. Pandey GP, Agrawal RC, Hashmi SA (2010) Electrical and electrochemical properties of magnesium ion conducting gel polymer electrolytes. *J Phys D Appl Phys* 43:255501–255506